Fibers and Polymers 2021, Vol.22, No.11, 2979-2985
DOI 10.1007/s12221-021-0019-9

ISSN 1229-9197 (print version)
ISSN 1875-0052 (electronic version)

Tannic Acid-chitosan Strengthened Cellulose Filter Paper for Water Disinfection via Formation of Silver Nanoparticles

Prena Chaudhary[1,2†], Kummara Madhusudana Rao[1†], Soon Mo Choi[1,2], Sunmi Zo[1], Maduru Suneetha[1], and Sung Soo Han[1,2*]

[1]*School of Chemical Engineering, Yeungnam University, Gyeongsan 38541, Korea*
[2]*Research Institute of Cell Culture, Yeungnam University, Gyeongsan 38541, Korea*
(Received January 6, 2021; Revised February 7, 2021; Accepted February 15, 2021)

Abstract: Materials containing silver nanoparticles (AgNPs) are of great interest for household uses, including drinking water disinfection. Although various Ag-containing materials are available, the development of low-cost, reusable, and durable systems is a challenge in water disinfection. Herein, we developed a low-cost, reusable, and durable cellulose filter paper (CFP) containing AgNPs decorated with a tannic acid (TA) and chitosan (CS) matrix (CFP-CSTAAg). The formation of CFP-CSTAAg composite was confirmed by FTIR, and XRD techniques. The formation of CSTAAg composite on CFP greatly improved the mechanical performance. CFP-CSTAAg is driven by gravity of 100 m*l* of a water sample containing *Staphylococcus aureus* for 30 min. The composite showed 99 % killing efficiency of bacteria as the bacteria cells did not pass through composite. The low-cost CFP-CSTAAg composite was reusable, providing a 98 % bacteria-killing capacity after five treatment cycles. The product's properties make reusable CFP-CSTAAg composite a promising filter for durable water disinfection as it is a low-cost material and eco-friendly.

Keywords: Cellulose filter paper, Tannic acid, Chitosan, Silver nanoparticles, Water disinfection

Introduction

The removal and inactivation of water containing pathogenic microorganisms is of utmost importance for developing safe and efficient products for human use [1]. Currently, the removal of organochloro compounds via chlorination-based disinfection methods to inactivate microbial pathogens has been used for drinking water purification. Due to the harmful nature of organochloro compounds, alternative methods are necessary to achieve effective removal of pollutants from contaminated water [2]. A filtration technique based on a size-exclusion mechanism can provide safe drinking water via the removal of particles and microbes of specific sizes [3]. Cost-effective and environmentally friendly cellulose-based filter papers (CFP) may be used to remove colloidal particles, but microbes are typically smaller and, thus, the most difficult to remove by size exclusion methods alone. However, CFP coated with electrostatic biopolymers or synthetic polymers have been used to filter microbes via the coating's creation of a net positive charge [4]. Additionally, the incorporation of AgNPs into CFP benefits bacterial inactivation due to their excellent intrinsic properties, including small size, spherical shape, high surface area, and high dispersion capacity [5].

Tannic acid (TA) is a natural polyphenolic acid extracted from plants. Structurally, hydroxyl groups are combined to one or more galloly residues in the chemical structure of TA [6,7]. TA has been studied for outstanding characteristics of anti-cancarcinogenic, anti-mutagenic, and ant-oxidant [8]. Moreover, it shows excellent inhibition capacity to against lungs, skin, fore stomach tumors caused by carcinogenic substance and environmental pollutants [9-11]. Recently, TA acts as a good reducing agent as well as stabilizing agent, in addition controlled the size of metal nanoparticles [12]. The combination of TA and metallic silver nanoparticles has shown excellent antibacterial properties and be applied in wound dressing applications [13].

Chitosan (CS), a partially deacetylated chitin is one of the second most abundant polysaccharide obtained from exoskeleton of crustacean shells. It is a non-toxic and biodegradability nature with copolymer of β-(1,4)-2-acetamido-2-deoxy-D-glucose and β-(1,4)-2-anaino-2-deoxy-D-glucose units [14]. Each glucosamine unit contains amino groups, and these groups are responsible for generation of positive charge which gives excellent properties of CS, its useful in pharmaceuticals, biotechnology, biomedical, biochemistry, cosmetic, food, paper and textile industries [15]. Also it has been used as an adsorbent due to the presence of functional groups are hydroxyl and amine in CS, these functional groups are easily bind and engage metal ions from aqueous solution. Metal ions are bind on polymer matrix via electrostatic and dipole-dipole interactions [16]. In recent years, the antibacterial CS has been widely studied and applied in antibacterial wound dressing and water purification applications [17]. The combination of CS with metallic nanoparticles also proven the improved biological performance of materials [18]. Additionally, due to availability of amino groups, CS can be easily modified in different ways to obtain crosslinked with other polymers or molecules, to meet various applications [19].

The development of a low-cost, reusable, and durable CFP

*Corresponding author: sshan@yu.ac.kr
†These authors contribute equally to this work.

containing AgNPs is tremendously interesting for application for household point-of-use drinking water disinfection. Herein, we describe the preparation of an eco-friendly, cost-effective, and efficient CFP containing AgNPs that include a tannic acid (TA) and chitosan (CS) matrix. The TA was chosen to result in a green reduction of Ag^+ ions within the AgNPs because the phenolic compound can quickly reduce Ag^+ ions via the formation of quinones [20]. It is hypothesized that a Schiff's base bond develops between the quinones of TA and the amino groups of CS, resulting in the strengthening of the CFP through the application of the CSTA matrix. The developed CFP-CSTAAg composite provided an improvement in CFP recycling capacity when used to remove pathogenic microorganisms from contaminated water.

Experimental

Materials

CS (deacetylation 84 %; medium molecular weight: 190,000-310,000), TA, silver nitrate ($AgNO_3$) were purchased from Sigma-Aldrich chemicals Co. Double distilled water (DDW) was used to prepare the solutions for this study. All other chemicals were used as received.

Fabrication of CFP-CSTAAg Composite

CFP was soaked in CS (medium molecular weight; deacetylation 84 %; Sigma-Aldrich Chemicals) solution (1 wt% CS in a 2 % acetic acid solution) and air-dried for one day to form CFP-CS. The CFP-CS was then immersed in $AgNO_3$ (Sigma-Aldrich Chemicals) solution (5 mM), and the Ag^+ ions became anchored to the CS functional groups. The Ag ions were reduced to form nanoparticles (AgNPs). The Ag^+-loaded CFP-CS was then dipped in a TA (Sigma-Aldrich Chemicals) solution for two hours. The Ag^+- CS- and TA-loaded CFP was designated as CFP-CSTAAg. In addition, CFP was coated with CS and TA using the same procedure but without the addition of Ag ions.

Characterization

The various coated CFPs (i.e., CFP, CFP-TA, CFP-CS, CFP-CSTA, and CFP-CSTAAg) were characterized by using ATR-FTIR (Perkin Elmer) at Core Research Support Center For Natural Products and Medical Materials (CRCNM) in Yeungnam university. The scan spectra of the samples were obtained over a range of 4000-450 cm^{-1} with an average scan of 25 at a resolution of 4 cm^{-1}. The XRD. patterns were recorded over an angular 2θ range of 10 ° to 70 ° (Brucker AXS D8 ADVANCE; operating at 40 kV and 30 mA) with a CuKα radiation source l=1.54 Å. The FE-SEM and EDX. Assessments provided elemental mapping images of the coated CFP composites (CFP-CS, CFP-CSTA, and CFP-CSTAAg), which were recorded using JEOL. with an acceleration voltage of 5.0 kV. The samples were pretreated by coating with Pt at a low deposition rate. Mechanical properties of the coated CFP composites (wet condition) were tested using an Instron 3345 universal testing machine with 5 kN loading and a crosshead speed of 50 mm min^{-1}.

Water Disinfection Properties

The antibacterial activities of the coated CFP composites were measured by counting *Staphylococcus aureus* (Gram-positive) colony-forming units (CFU). The *S. aureus* were grown overnight, aseptically inoculated into nutrient broth (10 m*l*), and incubated for 16 h at 37 °C with movement at 150 r/min. The bacterial cells were collected by centrifugation at 2000 r/min and subsequently suspended in water. For preparation of the experimental contaminated water, 100 m*l* of a water-bacteria suspension containing 1×10^8 CFU/m*l* bacteria was prepared and passed through CFP and the coated CFP composites. The effluent water samples were placed on agar plates, and the plates incubated overnight at 37 °C. The bacterial CFU were counted to determine the

Table 1. FTIR assignments of CFP treated with CS, TA, CSTA, and CSTAAg

CFP	CFP-CS	CFP-TA	CFP-CSTA	CFP-CSTAAg	Assignment
3328 cm^{-1} and 1635 cm^{-1}	3328 cm^{-1} and 1635 cm^{-1}	3328 cm^{-1} and 1635 cm^{-1}	3328 cm^{-1} and 1635 cm^{-1}	3328 cm^{-1} and 1635 cm^{-1}	-OH stretching and bending vibrations respectively (CFP)
1160 cm^{-1} and 1029 cm^{-1}	1160 cm^{-1} and 1029 cm^{-1}	1160 cm^{-1} and 1029 cm^{-1}	1160 cm^{-1} and 1029 cm^{-1}	1160 cm^{-1} and 1029 cm^{-1}	C-O (anti-symmetrical) and C-O-C bridges (CFP)
2902 cm^{-1}, 1315 cm^{-1}, and 1429 cm^{-1}	2902 cm^{-1}, 1315 cm^{-1}, and 1429 cm^{-1}	2902 cm^{-1}, 1315 cm^{-1}, and 1429 cm^{-1}	2902 cm^{-1}, 1315 cm^{-1}, and 1429 cm^{-1}	2902 cm^{-1}, 1315 cm^{-1}, and 429 cm^{-1}	C-H stretching and bending, as well as to the scissoring motions of CFP
	1650 cm^{-1}, 1580 cm^{-1}, and 1345 cm^{-1}		1650 cm^{-1}, and 1580 cm^{-1}		Stretching vibrations of amide I (acetylated), and II (-NH), respectively (CS polysaccharide)
		1716 cm^{-1}	1716 cm^{-1}	1716 cm^{-1}	Due to polyphenol (ester) stretching vibrations (TA)
				1640 cm^{-1}	C=N stretching vibrations

water disinfection properties of the coated CFP composites.

Results and Discussion

Fabrication of CFP-CSTAAg Composite

The Scheme 1 represents the method of formation of the CFP-CSTAAg nanocomposite. Initially, CS polymer chains were uniformly coated on cellulose fibers. After the addition of the $AgNO_3$ solutions, most of the Ag^+ ions became affixed to the CS. Finally, the addition of TA reduced the Ag^+ ions to AgNPs via the transformation of catechol to quinones. The resulting quinone moieties on TA were chemically involved in forming a Schiff base reaction with amino groups of CS, thereby strengthening the network structure of CS and the cellulose fibers of the CFP.

Characterization

The formation of Schiff's base was confirmed by examining the FTIR spectra. As from Figure 1a, the FTIR spectra of CFP includes an absorption band at 3328 cm^{-1} and one at 1635 cm^{-1} due to stretching and bending vibrations of O-H. The peaks at 2902 cm^{-1}, 1315 cm^{-1}, and 1429 cm^{-1} are attributed to C-H stretching and bending, as well as to the scissoring motions of CFP. The CFP shows stretching vibrations at 1160 cm^{-1} and 1029 cm^{-1}, representing the C-O (anti-symmetrical) and C-O-C bridges, respectively. The major peaks observed at 3430-3350 cm^{-1} due to H-bonded -OH and -NH stretching vibrations of CS. The peaks at 843 cm^{-1} and 1148 cm^{-1} were assigned to saccharide groups of CS. The important peaks at 1650, and 1580 cm^{-1} belongs to the stretching vibrations of amide I, and II (amine) respectively [21]. The FTIR spectra of TA shows intense band at 1716 cm^{-1} is due to polyphenol stretching vibrations. The peaks at 1612, 1535, and 1447 cm^{-1} were assigned to benzyl stretching vibrations. A peak at 759 cm^{-1} is due to trisubstituted benzene ring scissoring vibrations [22]. The cellulose functional groups were retained after coating by polymers and AgNPs with CFP. Furthermore, the new absorption peak at 1640 cm^{-1} was attributed to C=N stretching vibrations, as was confirmed by the reaction between TA and CS [23]. CFP has cellulose I peaks at 2θ of 14.8, 16.2, 22.5, and 34.3 ° attributed to the planes of (110), (110), (200), and (004) (Figure 1b) [24]. The XRD patterns of CFP-TA, CFP-CSTA, and CFP-CSTAAg were similar to that of CFP, suggesting that the coated CFP composites retained the crystalline structure of CFP (75 % crystallinity and 6.97 nm crystallite size) (Figure 1c). The retention of the CFP structure is crucial for the durability of applications in water disinfection, particularly when reusing the CFP material. Further, CFP-CSTAAg showed additional peaks at 2θ of 38.1, 44.4, 64.9, and 77.5, which were attributed to the presence of (111), (200), (220) and (311) phases that were the result of the successful formation of AgNPs with an fcc crystal structure (a=4.0790 Å) in the CFP-CSTA material (Figure 1c) [25].

Mechanical Properties

Figure 2 presents the tensile stress-strain curves for the

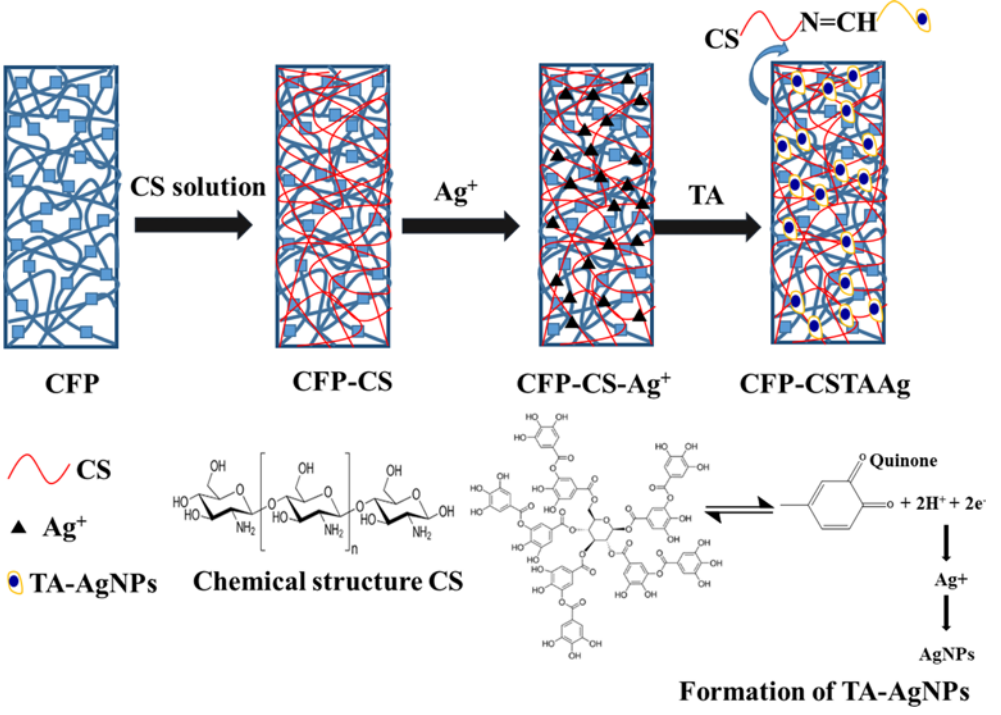

Scheme 1. Schematic representation of the formation of the CFP-CSTAAg nanocomposite.

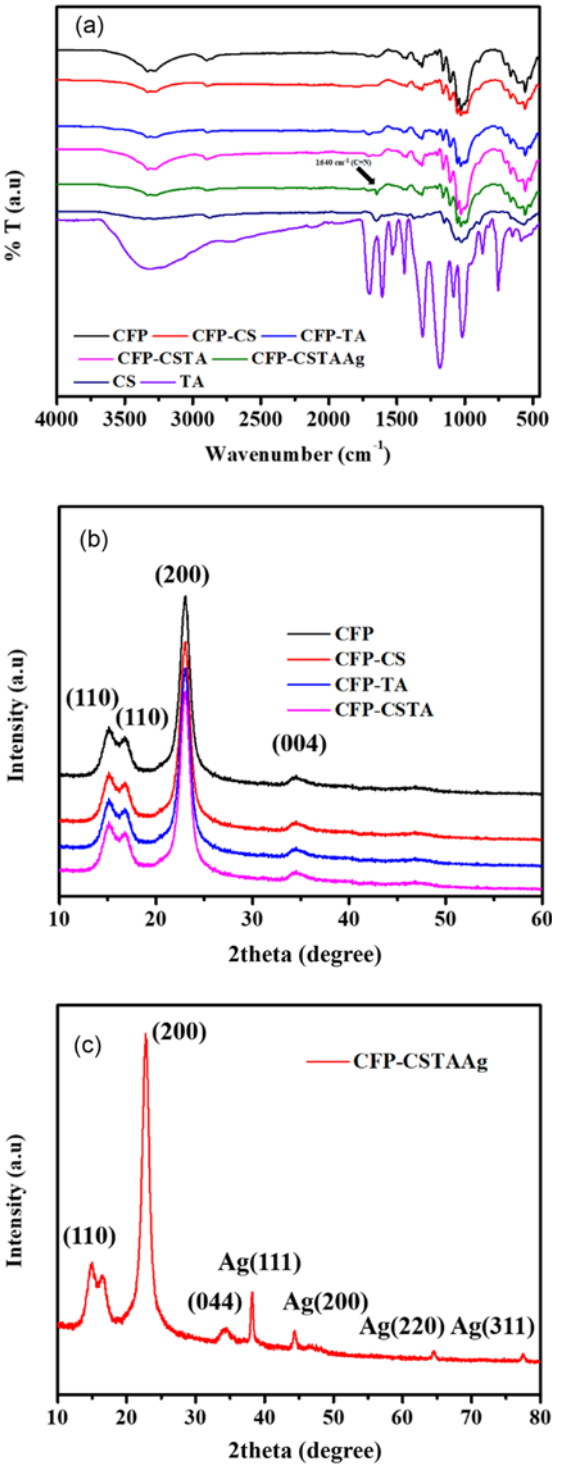

Figure 1. (a) FTIR spectra and (b, c) XRD patterns of CFP, CS-, TA-, CSTA-, and CSTAAg-coated CFPs.

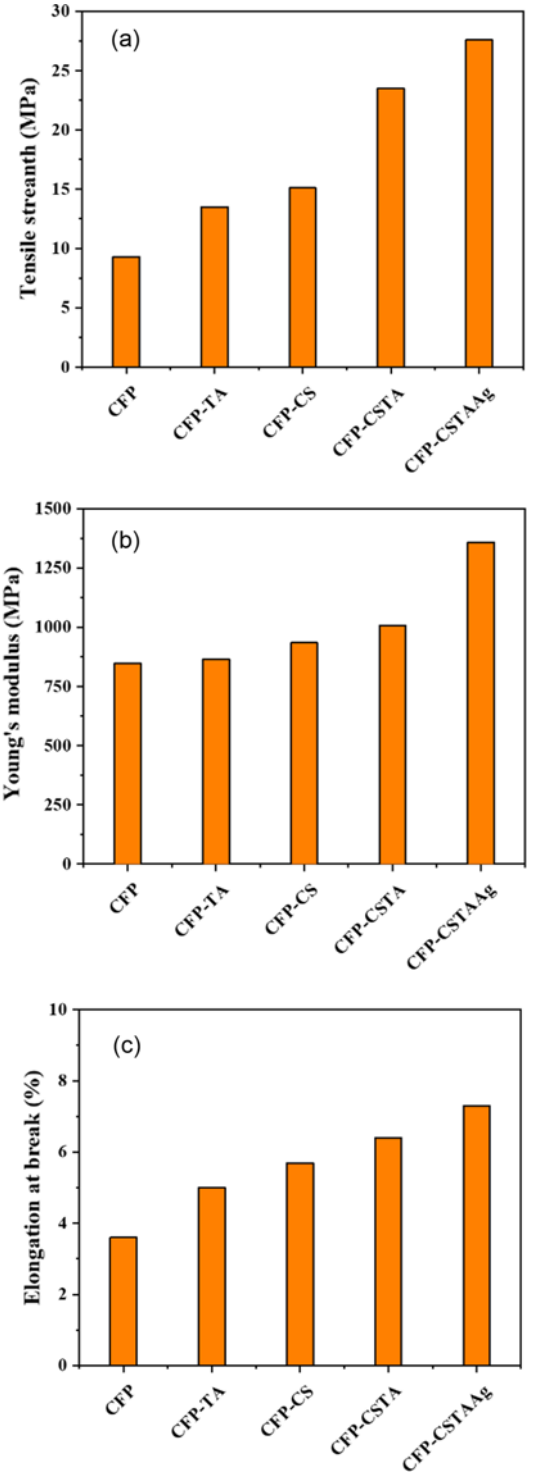

Figure 2. Mechanical properties of CFP, CS-, TA-, CSTA-, and CSTAAg-coated CFPs.

CPF coated with TA, CS, CSTA, and CSTAAg. The summary data include the mechanical properties such as maximum stress, Young's modulus, and percent elongation at breakage of all coated CFP composites. The results indicate that the CFP-CSTAAg composite had excellent mechanical properties and, therefore, could be utilized over

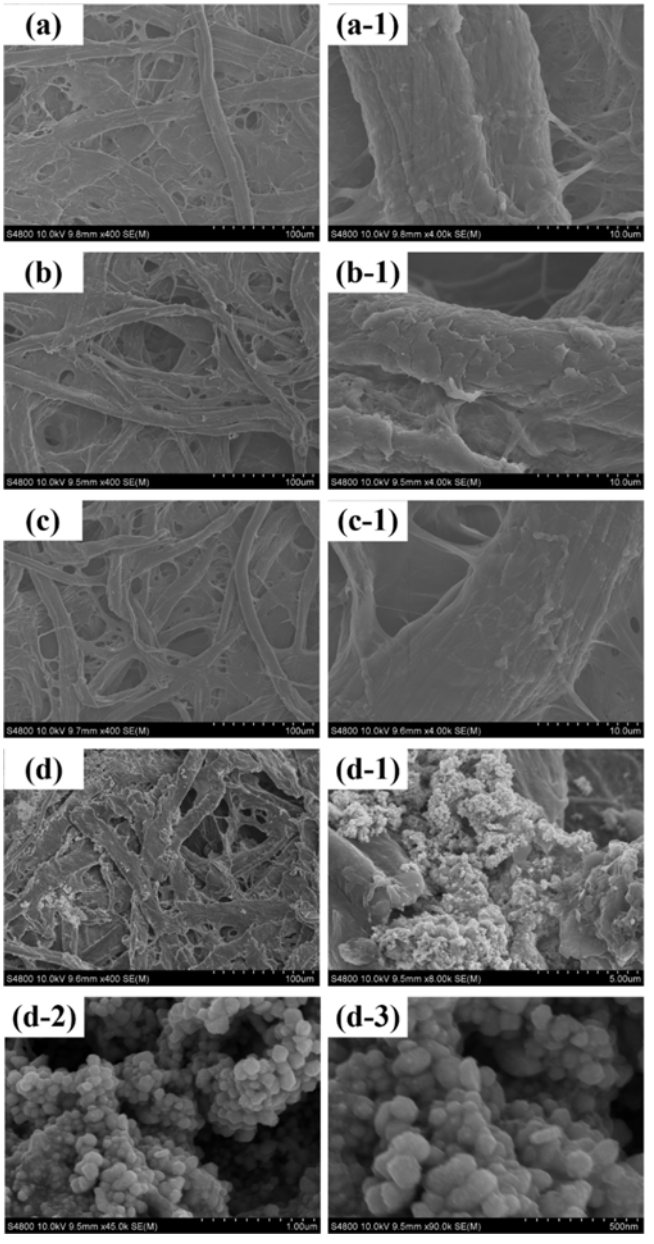

Figure 3. SEM images of (a, a-1) CFP-CS, (b, b-1) CFP-TA, (c, c-1) CFP-CSTA, and (d, d-1, d-2, d-3) CFP-CSTAAg.

a long duration without any significant damage or breakage due to TA and CS network structure that had formed along the cellulose fibers.

Morphology

Figure 3(a, a-1), (b, b-1), (c, c-1) shows various magnified FE-SEM images of the CFP-CS, CFP-TA, CFP-CS-TA matrices. Figure 3d, d-1, d-2, and d-3 shows the FE-SEM images of the CFP-CSTA-AgNPs. The pristine CFP is shown to be fibrous with a porous structure. Figure 3a, a-1, b, b-1 illustrates the CFP flat surface without a porous

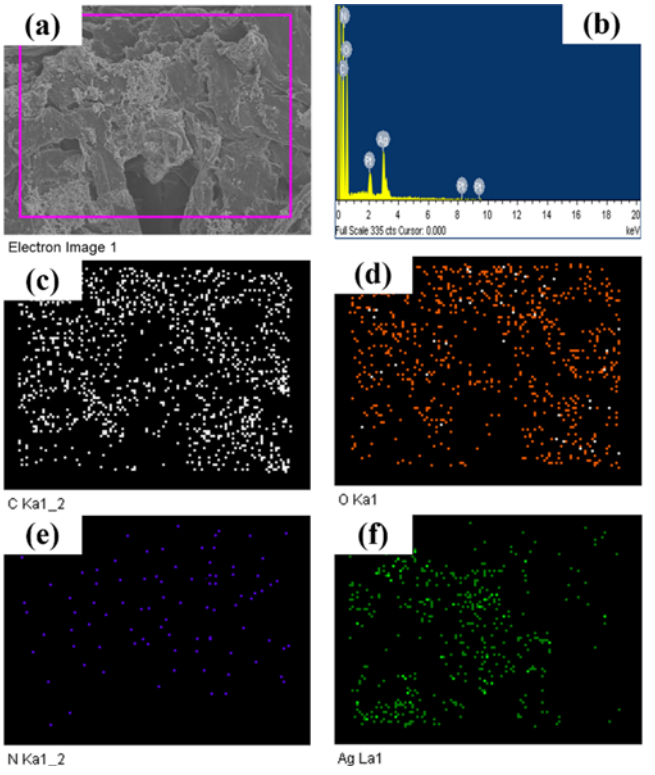

Figure 4. (a, b) SEM-EDX pattern and (c-f) SEM-EDX elemental mapping (C, N, O, Ag) of CFP-CSTAAg.

structure due to CS being coated on the CFP surface; moreover, the CFP morphology was unaffected by TA. CFP-CSTA (Figure 3c, c-1) is shown to have a smooth surface without morphological changes compared to that of the CFP-CS matrix. It was concluded that TA did not affect the morphology of the CFP-CS matrix. The aggregated molecules observed in Figure 3(d, d-1) corresponds to the AgNPs deposited in the CFP-CSTA matrix. The higher magnification image in Figure 3(d-2, d-3) shows the aggregated particles of AgNPs, clearly revealing the spherical structures when viewed under high magnification. The AgNPs observed on the surface of CFP-CSTA were due to the presence of TA reducing the Ag^{+} ions to AgNPs and stabilizing the AgNPs on the matrix, which was achieved by employing an *in situ* method. Figure 4(a-f) presents EDS images of the CFP-CSTAAg matrix and reveals the elemental existence of C, N, O, and Ag in CFP-CSTAAg.

Water Disinfection

A simple filtration setup with an *S. aureus* bacterial suspension in water (10^5 CFU/m*l*) was used to test the disinfection performance of the coated CFP composites. Representative results of the percentage bacterial viability of *S. aureus* in the effluent from the various CFPs are shown in Figure 5a. The percent viability of *S. aureus* after percolating through CFP-TA and CFP-CSTA was 5 % and

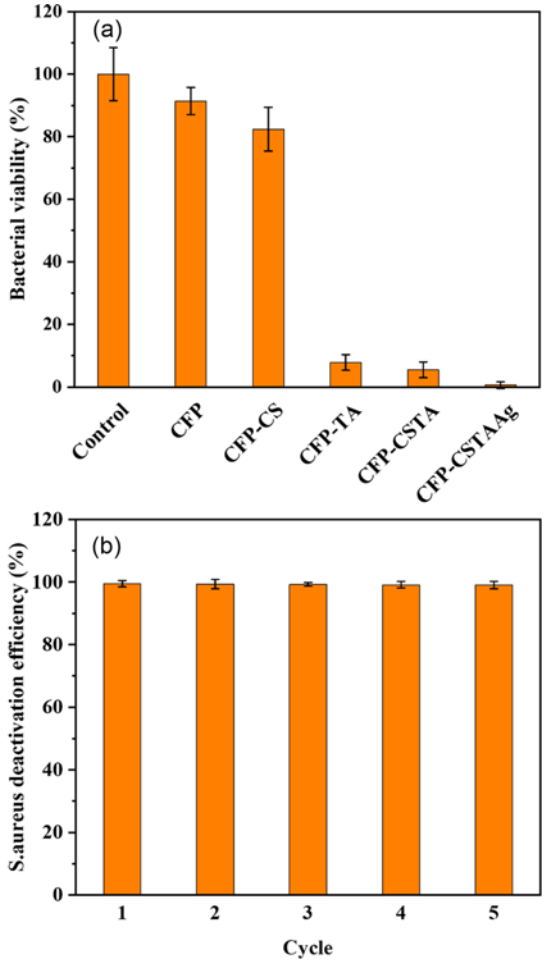

Figure 5. (a) Bacterial viability of CFP, CS-, TA-, CSTA-, and CSTAAg-coated CFPs against *S. aureus* and (b) bacterial inactivation efficiency of CFP-CSTAAg.

4.5 %, respectively. The addition of AgNPs to the CFP-CSTA network further reduced the percent viability of *S. aureus*. The antibacterial action is attributed to the presence of AgNPs and TA molecules in the CFP. The AgNPs can easily be involved the disruption of the signal transduction of bacteria, which leads to cause of bacterial cell death [26]. Owing to the presence of a CSTA network, the CFP has increased durability allowing reuse of the CFP. The CFP-CSTAAg after five consecutive filtrations of *S. aureus* in water resulted in 99 % bacterial inhibition, demonstrating both the durability and reusability of the CFP-CSTAAg composite for disinfection of bacteria-contaminated water.

Conclusion

In this work, a low-cost, reusable, and durable cellulose filter paper (CFP) containing AgNPs decorated with a tannic acid (TA) and chitosan (CS) matrix (CFP-CSTAAg) was developed. The CFP, when coated with TA, CS, CSTA, or CSTAAg, retained its crystalline structure, and the coatings provided improved mechanical performance. The AgNPs incorporated into the CFP-CSTA composite provided a bacteria-killing rate of 99 %. The CFP-CSTAAg composite was reusable and provided a 98 % bacteria-killing rate after five reuses. Thus, the developed reusable CFP-CSTAAg composite, produce with low-cost materials and using environmentally friendly methods, has the potential for use and reuse in water disinfection.

Acknowledgements

This work was financially supported by the National Research Foundation of Korea (NRF) [grant numbers 2019R1I1A3A01063627, 2020R1A6A1A03044512, 2020R1A6A3A01100150]. This work was also supported by the 2015 Yeungnam University Research Grant.

References

1. F. Bashir, M. Irfan, T. Ahmad, J. Iqbal, M. T. Butt, Y. Sadef, M. Umbreen, I. A. Shaikh, and M. Moniruzzaman, *Environ. Technol. Innov.*, **21**, 101228 (2020).
2. S. Kumar, A. K. Gupta, A. Maurya, and M. K. Singh in "Waterborne Pathogens" (M. N. V. Prasad and A. Grobelak Eds.), pp.205-218, Butterworth-Heinemann, 2020.
3. A. C. C. Rotzetter, C. R. Kellenberger, C. M. Schumacher, C. Mora, R. N. Grass, M. Loepfe, N. A. Luechinger, and W. J. Stark, *Adv. Mater.*, **42**, 6057 (2013).
4. S. Li, D. Wang, H. Xiao, H. Zhang, S. Cao, L. Chen, Y. Ni, and L. Huang, *Carbohydr. Polym.*, **255**, 117352 (2020).
5. C. A. Mecha and V. L. Pillay, *J. Membr. Sci.,* **458**, 149 (2014).
6. S. K. Sivaraman, I. Elango, S. Kumar, and V. Santhanam, *Curr. Sci.,* **97**, 1055 (2009).
7. X. Tian, W. Wang, and G. Cao, *Mater. Lett.,* **61**, 130 (2007).
8. S. A. Aromal and D. Philip, *Physica E.,* **44**, 1692 (2012).
9. Z. G. Huyut, M. Elmastas, and H. Y. Aboul-Enein, *Arab. J. Chem.,* **3**, 43 (2010).
10. R. E. Vance and R. W. Teel, *Cancer Lett.,* **47**, 37 (1989).
11. W. A. Khan, Z. Y. Wang, M. Athar, D. R. Bickers, and H. Mukhtar, *Cancer Lett.,* **42**, 7 (1988).
12. T. Ahmad, *J. Nanotechnol.,* **2014**, 954206 (2014).
13. H. Ye, J. Cheng, and K. Yu, *Int. J. Biol. Macromol.,* **121**, 633 (2019).
14. I. Younes and M. Rinaudo, *Mar. Drugs.,* **13**, 1133 (2015).
15. N. Morin-Crini, E. Lichtfouse, G. Torri, and G. Crini, *Environ. Chem. Lett.,* **17**, 26 (2019).
16. Y. Na, J. Lee, S. H. Lee, P. Kumar, J. H. Kim, and R. Patel, *Polym.-Plast. Tech. Mat.,* **59**, 1770 (2020).
17. M. Kong, X. G. Chen, K. Xing, and H. J. Park, *Int. J. Food Microbiol.,* **144**, 51 (2010).
18. C. A. dos Santos, A. P. Ingle, and M. Rai, *Appl. Microbiol.*

Biotechnol., **104**, 2373 (2020).
19. D. Nataraj, S. Sakkara, M. Meghwal, and N. Reddy, *Int. J. Biol. Macromol.,* **120**, 1256 (2018).
20. Y. Cao, R. Zheng, X. Ji, H. Liu, R. Xie, and W. Yang, *Langmuir,* **13**, 3876 (2014).
21. M. Suneetha, K. M. Rao, and S. S. Han, *Int. J. Biol. Macromol.,* **144**, 160 (2020).
22. C. Chen, X. W. Geng, Y. H. Pan, Y. N. Ma, Y. X. Ma, S. Z. Gao, and X. J. Huang, *RSC Adv.,* **10**, 1724 (2020).
23. L. Zhang, W. Tang, T. Ma, L. Zhou, C. Hui, X. Wang, P. Wang, C. Zhang, and C. Chen, *RSC Adv.,* **9**, 38935 (2019).
24. T. Kamal, S. B. Khan, S. Haider, Y. G. Alghamdi, and A. M. Asiri, *Int. J. Biol. Macromol.,* **104**, 56 (2017).
25. N. Zhang, J. Luo, R. Liu, and X. Liu, *RSC Adv.,* **6**, 83720 (2016).
26. A. Roy, O. Bulut, S. Some, A. K. Mandal, and M. D. Yilmaz, *RSC Adv.,* **9**, 2673 (2019).